

Long-lived optical phonons in ZnO studied with impulsive stimulated Raman scattering

C. Aku-Leh,¹ J. Zhao,¹ R. Merlin,¹ J. Menéndez,² and M. Cardona³

¹*FOCUS Center and Department of Physics, The University of Michigan, Ann Arbor, MI 48109-1120, USA*

²*Department of Physics and Astronomy, Arizona State University, Tempe, AZ, 85287-1504, USA*

³*Max-Planck-Institut für Festkörperforschung, Heisenbergstraße 1, 70569 Stuttgart, Germany*

(Received 10 March 2005; published 27 May 2005)

The anharmonic properties of the low-frequency E_2 phonon in ZnO were measured using impulsive stimulated Raman scattering. At 5 K, the frequency and lifetime are (2.9789 ± 0.0002) THz and (211 ± 7) ps. The unusually long lifetime and the high accuracy in the determination of the frequency hold promise for applications in metrology, quantum computation and materials characterization. The temperature dependence of the lifetime is determined by two-phonon upconversion decay contributions, which vanish at zero temperature. Results suggest that the lifetime is limited by isotopic disorder and that values in the nanosecond range may be achievable in isotopically pure samples.

DOI: 10.1103/PhysRevB.71.205211

PACS number(s): 63.20.Kr, 78.47.+p, 42.65.Dr, 63.20.Ry

I. INTRODUCTION

The development of commercial laser sources with femtosecond pulses has made it possible to generate and control coherent excitations in semiconductors.¹⁻³ This capability creates exciting opportunities for applications and provides a powerful tool for the study of fundamental interactions. In particular, detailed schemes have been proposed to take advantage of coherent fields for ultrafast optical-data processing which require long-lived excitations for information storage and vanishing group velocities for miniaturization.⁴ Recent impulsive stimulated Raman scattering (ISRS) experiments in wurtzite ZnO⁵ and GaN⁶ suggest that their doubly degenerate low-frequency (LF) E_2 phonons have exactly these properties. In ZnO, Lee and co-workers⁵ find a lifetime of $\tau=29.2$ ps at room temperature, about an order of magnitude longer than typical lifetimes for Raman phonons in semiconductors.⁷ Similarly, the corresponding E_2 mode in GaN was found to have a lifetime of $\tau=70$ ps.⁶ Long-lived optical phonons are potentially of interest for applications in quantum information science. In particular, doubly and triply degenerate modes could play a role similar to that of photons in quantum cryptography⁸ and, like photons in cavity-quantum-electrodynamics schemes for quantum computing,⁹ phonons could also be drawn to mediate the interaction between qubits. Within this context, we note that phonons associated with the center-of-mass motion of a system of trapped ions have been utilized to mediate their interaction and produce many-particle entangled states.^{10,11}

In this paper, we report an ISRS study of the temperature dependence of the frequency and lifetime of the lowest-lying E_2 phonon in ZnO, referred to in the following as E_2 (LF). We find a dramatic lifetime increase as the temperature is decreased, up to a value of $\tau=211$ ps at 5 K. This strong temperature dependence is explained in terms of an anharmonic decay mechanism dominated by phonon upconversion processes. The upconversion contribution to the phonon lifetime is expected to vanish as the temperature approaches zero, and indeed our measured low-temperature lifetime is close to the predicted lifetime due to isotopic disorder in

natural ZnO. Hence we expect isotopically pure ZnO crystals to have even longer phonon lifetimes, probably in the nanosecond range. Our study also reveals that the frequency of long-lived phonons detected with ISRS can be determined with a precision of a few parts per million. On that account ISRS of long-lived phonons may have additional applications in metrology (although the quality factor for ZnO is ~ 2000 , i.e., 1–2 orders of magnitude below those for quartz oscillators,¹² which, however, operate at much lower frequencies), as well as for characterizing the purity and perfection of semiconductor crystals.

II. EXPERIMENTAL

Measurements were performed on a $10 \times 5 \times 1$ mm³ ZnO single crystal, with the c axis parallel to the larger side of the parallelepiped, in the temperature range 5–300 K using a continuous-flow liquid-He optical cryostat. Pressures were kept constant at ~ 28 kPa. The laser was a regenerative amplifier seeded by a Ti:Sapphire oscillator providing ~ 70 fs pulses of central wavelength 803 nm at 250 kHz [note that, although ~ 5 times larger than the E_2 (LF) frequency, the pulse bandwidth is too small to observe oscillations associated with the second E_2 phonon at ~ 13.3 THz⁵]. Since the laser energy is well below the band gap of ZnO, the generation mechanism of coherent phonons is ISRS.² Data were obtained using a conventional pump-probe setup. The pump pulse creates coherent vibrations, which modulate temporally and spatially the refractive index of the material. In turn, this modulation leads to a change in the transmission of the probe beam, $\delta T(\omega)$, which we measured as a function of the light frequency ω and the delay between the two pulses using standard lock-in methods. Because the photon number is conserved in ISRS, i.e., $\int_{-\infty}^{+\infty} \delta T = 0$,² we measured $\Delta T \equiv (\int_{-\infty}^{\omega_C} \delta T - \int_{\omega_C}^{+\infty} \delta T)$ using a grating to disperse and a balanced detector to determine the difference between the two halves of the spectrum; ω_C is the central frequency of the pulses. To satisfy the selection rules for E_2 phonons, the pump and probe polarization were both parallel to the a axis. Light penetrated the largest face of the crystal through a

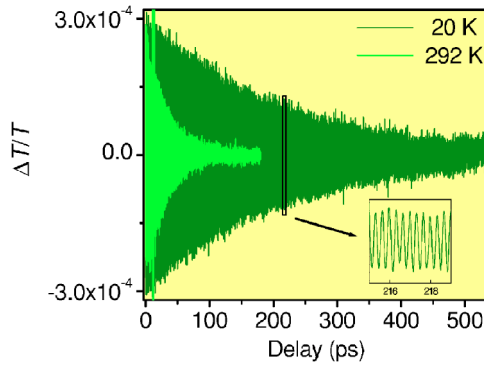


FIG. 1. (Color online). Differential change in transmission at 20 K and 292 K showing coherent E_2 (LF) oscillations in ZnO. The black rectangle indicates the range of the scan shown in the inset.

circular spot of diameter $66 \mu\text{m}$ (pump) and $38 \mu\text{m}$ (probe), using an average power of 10 mW (pump) and 2.5 mW (probe).

III. RESULTS

In Fig. 1 we show an example of coherent phonon oscillations associated with E_2 (LF). For a strictly impulsive force, $\delta(t)$, a mode of frequency f_0 behaves as $Q \propto e^{-\Gamma t} \sin(2\pi f_0 t)$, where Q is the phonon coordinate and $\Gamma = 1/\tau$.¹³ Since $\Delta T \propto dQ/dt$,² we get $\Delta T \propto e^{-\Gamma t} \cos(2\pi f_0 t)$. Thus, it is, in principle, possible to relate the *real* part of the Fourier transform (FT) of the transmitted signal to the spontaneous Raman line shape, determined by the imaginary part of the phonon self-energy.^{2,14} However, uncertainty in the determination of time zero and artifacts produced by multiple reflections of the pump beam cause the FT components to become a mixture of the real and imaginary parts of the self-energy. This problem could be partially circumvented by computing the power spectrum, but such approach is not entirely satisfactory because the width of the power spectrum is not directly related to the width of the imaginary part of the self-energy. To solve this problem, we developed a phase-correction algorithm similar to the one used for the analysis of nuclear-magnetic-resonance (NMR) data.¹⁵ This algorithm yields a corrected FT spectrum that can be directly compared with theoretical calculations of the Raman line shape. In Fig. 2 we show the corrected FT of the coherent phonon oscillations, which we denote as the Raman line shape. In addition to applying the above-mentioned phase correction, we optimized the density of points in Fig. 2 by using a standard NMR-FFT (fast FT) zero-filling approach.⁹ We fit the resulting line shape with a Lorentzian profile of the form $A[(f-f_0)^2 + (\Gamma/2\pi)^2]^{-1}$, from which we obtain the mode frequency f_0 and the full width at half maximum $\text{FWHM} = \Gamma/\pi$ of the Raman line shape. These parameters are plotted in Fig. 3 as a function of temperature. Notice the high precision of the data. For $T=5$ K, for example, the mode frequency is $f_0 = (2.9789 \pm 0.0002)$ THz [(99.390 ± 0.007) cm^{-1}] and $\Gamma/\pi = (1.602 \pm 0.052) \times 10^{-3}$ THz [(0.0535 ± 0.002) cm^{-1}].

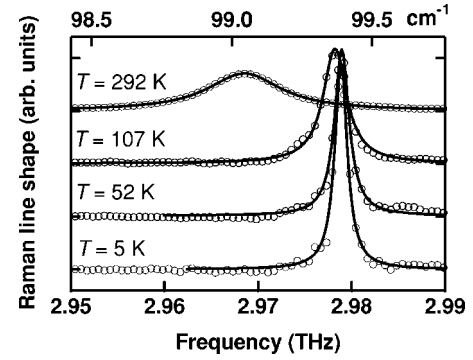


FIG. 2. Raman line shapes obtained from the time-domain coherent phonon oscillations (circles). The solid lines represent Lorentzian fits to the data. An arbitrary vertical offset was applied to the data for clarity.

Thus the frequency is obtained with five significant figures.¹⁶ The largest source of error in the frequency is the uncertainty in the length of the delay line, followed by corrections arising from fluctuations in the refractive index of air. Since there are relatively simple ways to reduce the experimental uncertainty, the ultimate precision of the ISRS technique has not been reached so far. The ability to measure phonon frequencies with very high precision may open up applications for phonon spectroscopy in materials.

In order to validate our FT procedure, we also obtained the lifetimes directly from the time-domain data by fitting 4 ps segments of data (see the inset of Fig. 1) with an expression of the form $A \cos(2\pi f_0 t + \alpha)$ and plotting the resulting average amplitude A versus the average delay time t_c (the time at the center of the interval), as shown in Fig. 4.

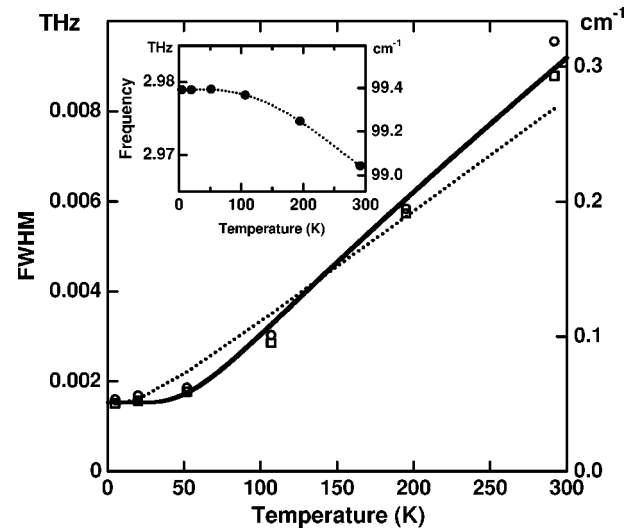


FIG. 3. Temperature dependence of the Raman line shape FWHM obtained from Lorentzian fits to the frequency-domain data (circles) and time-domain fits to the coherent-oscillation amplitude using a simple decaying exponential (squares); see the text and also Fig. 4. The diameter of the circles and the side of the squares give the vertical errors. Full and dotted lines are fits neglecting, respectively, down- and up-conversion processes. Inset: frequency versus temperature. The dotted curve is a guide to the eye.

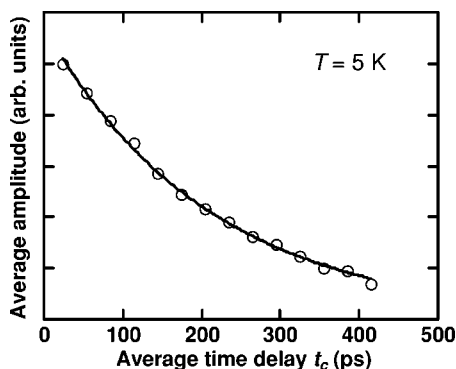


FIG. 4. Average oscillating amplitude over 4 ps segments as a function of the average delay time for the segment. The solid line represents the best fit with a single decaying exponential.

The $A(t_c)$ curve is then fitted with a single exponential $B \exp(-\Gamma t_c)$, from which Γ can be extracted. The results are plotted as squares in Fig. 3. As expected, the broadening parameters obtained from the time domain analysis are nearly the same as those obtained from the frequency domain fits. Notice that the value of the lifetime at room temperature, $\tau = \Gamma^{-1} = 34.1$ ps, is somewhat longer than 29.2 ps, as reported in Ref. 5.

The temperature dependence of the linewidth of the Raman line shape is usually fitted using^{17,18}

$$\Gamma(T) = \Gamma_0 + \Gamma_{\text{DN}}(1 + n_1 + n_2), \quad (1)$$

where $n_{1,2} = [\exp(hf_{1,2}/k_B T) - 1]^{-1}$ is the phonon occupation number and the frequencies satisfy $f_1 + f_2 = f_0$. The term Γ_0 accounts for a temperature-independent broadening caused by defects, including isotopic mixture. The second term on the right-hand side models a phonon *downconversion* process induced by third-order anharmonicity. It represents the decay of the optical mode into two lower-frequency phonons. The downconversion term is actually an appropriately weighted sum over all allowed decay channels^{19,20} satisfying the conservation of energy and crystal momentum. Equation (1) replaces the sum over individual channels by a single effective decay channel. Recent *ab initio* predictions^{20–22} provide a strong justification for this approach, since they show indeed that the decay frequencies cluster around a few pairs (often only one pair) of values. The phonon occupation numbers vanish at low temperatures, and the downconversion contribution approaches a constant value Γ_{DN} . The magnitude of Γ_{DN} is determined by an anharmonic matrix element and the density of two-phonon states at the frequency f_0 of the decaying phonon. When this frequency is sufficiently low, the only possible decay products are combinations of acoustic phonons, whose density of states is a rapidly decreasing function of frequency. The anharmonic matrix elements also vanish in the low-frequency limit,²² so that the lifetime due to downconversion processes should increase sharply as the frequency f_0 decreases.

In ZnO, the E_2 (LF) frequency f_0 is much lower than the maximum optical phonon frequency of ~ 17.6 THz for the A_1 longitudinal-optical mode.²³ Therefore, we expect phonon

downconversion processes to make a small contribution to the phonon lifetime. On the other hand, the existence of phonon branches with frequencies *higher* than f_0 enables an additional third-order anharmonic process, mainly the decay of the Raman phonon with the simultaneous annihilation of a phonon of frequency f_3 and the creation of a phonon with frequency f_4 . By including these *up-conversion* processes, the expression for Γ becomes

$$\Gamma(T) = \Gamma_0 + \Gamma_{\text{DN}}(1 + n_1 + n_2) + \Gamma_{\text{UP}}(n_3 - n_4). \quad (2)$$

Notice that the upconversion term vanishes at zero temperature, so that even with the inclusion of this term the low-temperature lifetime in defect-free materials should be dominated by downconversion processes. To the best of our knowledge, the upconversion contribution to the anharmonic decay of Raman-active phonons in semiconductors has never been conclusively detected. In particular, the Raman-active longitudinal-optical phonons in most cubic semiconductors have the highest vibrational frequency in the crystal, and therefore the upconversion process is forbidden for these phonons. The predominance of the upconversion channel has been recently established in measurements of the lifetime of the TA (X) phonons in Ge and confirmed by *ab initio* calculations.²⁴

Given the different behaviors for $T \rightarrow 0$, a fit with Eq. (2) can easily establish the relative weight of the down- and upconversion channels if the defect contribution can be neglected. Unfortunately, our ZnO sample possesses a natural distribution of Zn and O isotopes, so that the first term in Eq. (2) cannot be neglected. A fit with the full Eq. (2) expression is difficult and leads to large errors in the fitting parameters. We therefore adopt the following approach. First, we fit the temperature dependence of the inverse lifetime by neglecting the upconversion contribution. For this, we assume $f_1 = f_2 = f_0/2$ (the so-called Klemens ansatz,²⁵ and we obtain the dotted line in Fig. 3, with $\Gamma_0/\pi = 0.0006$ THz and $\Gamma_{\text{DN}}/\pi = 0.0009$ THz. (A fit with $f_1 = x f_0$, $f_2 = (1-x)f_0$, with x an adjustable parameter as in Ref. 26, yields $x = 0.7$, but the curve is hardly distinguishable from the dotted line in Fig. 3. Next, we neglect the downconversion channel and fit the experimental results with an expression that contains only the first and third terms in Eq. (2). From inspection of the calculated phonon density of states (DOS) for ZnO,²³ we identify two possible sets of frequencies for the upconversion process: $f_3 = 13.4$ THz; $f_4 = 16.4$ THz and $f_3 = 4.47$ THz; $f_4 = 7.45$ THz. The first combination gives a poor fit, but the second one yields the solid line in Fig. 3, with parameters $\Gamma_0/\pi = 0.0015$ THz and $\Gamma_{\text{UP}}/\pi = 0.015$ THz. It is apparent from a comparison of the two curves in Fig. 3 that the upconversion fit is in better agreement with experiment. This strongly suggests that phonon upconversion processes play a dominant role in the anharmonic decay of the E_2 (LF) phonons in wurtzite materials. Our findings are consistent with the work on TA (X) phonons in Ge mentioned above, for which upconversion processes were found to dominate and the low-temperature lifetime estimated at 2 ns.²⁴ The E_2 (LF) phonons in the wurtzite structure are, in some sense, equivalent to TA (L) phonons in the zinc blende structure.

Since the kinematic decay restrictions for TA (L) and TA (X) are similar, the upconversion channel should also be dominant for TA (L) phonons in zinc blende as well as for E_2 (LF) phonons in wurtzite.

Theoretical estimates of the isotopic contribution to the linewidth of the E_2 (LF) phonon provide additional support for the dominance of upconversion processes. The corresponding phonon eigenvector consists mainly of Zn displacements, so it is the isotopic disorder in the Zn sublattice that affects the phonon lifetime. Our natural ZnO crystals contain 48.6% ^{64}Zn , 27.9% ^{66}Zn , 4.1% ^{67}Zn , 18.75% ^{68}Zn , and 0.6% ^{70}Zn ,²⁷ and therefore the isotopic contribution to Γ should be sizable. A recent calculation using *ab initio* phonon density of states yields $\Gamma_0/\pi=0.0018$ THz.²³ This is very close to the experimental value for the FWHM at low temperatures, suggesting that at these temperatures the intrinsic anharmonic linewidth is significantly small, as expected for an upconversion-dominated decay mechanism. This exciting result indicates that in isotopically pure samples the lifetime of the E_2 (LF) phonon could be an order of magnitude longer (and perhaps even longer) than in our natural crystals. Lifetimes in the nanosecond range have not yet been reported for optical phonons in semiconductors.

IV. CONCLUSIONS

In summary, we have shown that the E_2 (LF) phonon lifetime in ZnO is longer than 200 ps at low temperatures, and probably in the ns range in isotopically pure crystals. Long low-temperature E_2 (LF) lifetimes should also be expected in other wurtzite materials, including CdS, CdSe, GaN, and AlN. Moreover, more complex tetrahedral semiconductors (such as the chalcopyrite materials of the I-III-VI₂ family) display a number of optical phonon branches with even lower frequencies.²⁸ Hence these materials are also strong candidates for coherently driven long-lived optical phonons. Our results demonstrate the extraordinary potential of the ISRS technique, not only for anharmonicity studies, but also for new spectroscopic applications. Phonon frequencies determined with the precision that can be attained with ISRS should be sensitive to extremely small crystalline perturbations that hitherto were considered to be beyond the reach of phonon spectroscopy.

This work was supported by the AFOSR under Contract No. F49620-00-1-0328 through the MURI program and by the NSF Focus Physics Frontier Center. J. M. would like to acknowledge support through the NSF FOCUS Fellows program at the University of Michigan.

-
- ¹W. Sha, A. L. Smirl, and W. F. Tseng, *Phys. Rev. Lett.* **74**, 4273 (1995).
- ²R. Merlin, *Solid State Commun.* **102**, 207 (1997).
- ³M. U. Wehner, M. H. Ulm, D. S. Chemla, and M. Wegener, *Phys. Rev. Lett.* **80**, 1992 (1998).
- ⁴D. Mihailovic, D. Dvorsek, V. V. Kabanov, and J. Demsar, *Appl. Phys. Lett.* **80**, 871 (2002).
- ⁵I. H. Lee, K. J. Yee, K. G. Lee, E. Oh, D. S. Kim, and Y. S. Lim, *J. Appl. Phys.* **93**, 4939 (2003).
- ⁶K. J. Yee, K. G. Lee, E. Oh, D. S. Kim, and Y. S. Lim, *Phys. Rev. Lett.* **88**, 105501 (2002).
- ⁷F. Vallée, *Phys. Rev. B* **49**, 2460 (1994).
- ⁸D. Fattal, K. Inoue, J. Vuckovic, C. Santori, G. S. Solomon, and Y. Yamamoto, *Phys. Rev. Lett.* **92**, 037903 (2004), and references therein.
- ⁹T. Pellizzari, S. A. Gardiner, J. I. Cirac, and P. Zoller, *Phys. Rev. Lett.* **75**, 3788 (1995).
- ¹⁰C. A. Sackett, D. Kielpinski, B. E. King, C. Langer, V. Meyer, C. J. Myatt, M. Rowe, Q. A. Turchette, W. M. Itano, D. J. Wineland, and C. Monroe, *Nature (London)* **404**, 256 (2000).
- ¹¹F. Schmidt-Kaler, H. Häffner, M. Riebe, S. Gulde, G. P. T. Lancaster, T. Deuschle, C. Becher, C. F. Roos, J. Eschner, and R. Blatt, *Nature (London)* **422**, 408 (2003).
- ¹²See, e.g., M. Hieda, R. Garcia, M. Dixon, T. Daniel, D. Allara, and M. H. W. Chan, *Appl. Phys. Lett.* **84**, 628 (2004), and references therein.
- ¹³ Γ includes contributions of elastic and inelastic scattering processes which ISRS cannot separate. Since the E_2 (LF) phonon is an extended mode and the disorder usually present in high-quality semiconductors, particularly isotope disorder, is too weak to induce localization, it is not very meaningful to describe decay as a sum of homogeneous and inhomogeneous terms. Also note that both anharmonic and disorder scattering couple Raman phonons to continua.
- ¹⁴A. S. Barker, Jr. and R. Loudon, *Rev. Mod. Phys.* **44**, 18 (1972).
- ¹⁵J. D. Roberts, *ABCs of FT-NMR* (University Science Books, Sausalito, 2000).
- ¹⁶The reason why the error in the frequency is significantly smaller than $\Gamma/\pi f_0$ is that the phase of the oscillations is known with a precision better than $\sim 2\pi \times 10^{-2}$; see: D. B. Percival and A. T. Walden, *Spectral Analysis for Physical Applications* (University Press, Cambridge, 1993).
- ¹⁷R. F. Wallis and M. Balkanski, *Many Body Aspects of Solid State Spectroscopy* (North-Holland, Amsterdam, 1986).
- ¹⁸J. Menéndez, in *Raman Scattering in Materials Science*, Springer Series in Materials Science, edited by W. H. Weber and R. Merlin (Springer, Berlin, 2000), Vol. 24, p. 55.
- ¹⁹R. A. Cowley, *Proc. Phys. Soc. London* **84**, 281 (1964).
- ²⁰A. Debernardi, S. Baroni, and E. Molinari, *Phys. Rev. Lett.* **75**, 1819 (1995).
- ²¹A. Debernardi, *Phys. Rev. B* **57**, 12 847 (1998).
- ²²A. Debernardi, *Solid State Commun.* **113**, 1 (2000).
- ²³J. Serrano, A. H. Romero, F. J. Manjón, R. Lauck, M. Cardona, and A. Rubio, *Phys. Rev. B* **69**, 094306 (2004).
- ²⁴J. Kulda, A. Debernardi, M. Cardona, F. de Geuser, and E. E. Haller, *Phys. Rev. B* **69**, 045209 (2004).
- ²⁵P. G. Klemens, *Phys. Rev.* **148**, 845 (1966).
- ²⁶J. Menéndez and M. Cardona, *Phys. Rev. B* **29**, 2051 (1984).
- ²⁷K. J. R. Rosman and P. D. P. Taylor, *Pure Appl. Chem.* **70**, 217 (1998).
- ²⁸J. Gonzalez, L. Roa, R. Fouret, P. Derollez, J. Lefebvre, and Y. Guinet, *Phys. Status Solidi B* **225**, R12 (2001).